THE JOURNAL OF PHYSICAL CHEMISTRY C

Article

pubs.acs.org/JPCC

Mechanism of Label-Free DNA Detection Using the Floating Electrode on Pentacene Thin Film Transistor

Min-Ho Park,[†] Dawoon Han,[†] Rohit Chand,* Dong-Hoon Lee, and Yong-Sang Kim*

School of Electronic and Electrical Engineering, Sungkyunkwan University, Suwon, Gyeonggi 440-746, South Korea

Supporting Information

ABSTRACT: The analysis of DNA in the posthuman genome project era has become an ever-expanding branch of research and is thus routinely employed in the majority of biochemical laboratories. This work discusses the mechanism and label-free detection of DNA using a pentacene thin film transistor with a gold floating electrode on the active layer. Thiolated polynucleotide probes were used, which form self-aligned monolayers on the floating electrode over the pentacene active layer. The immobilization of the DNA on floating electrode increased the work function and raised the Schottky barrier of the device, resulting in a charge screening effect. Hence, the negative charge of the DNA caused a positive shift in the threshold voltage of the transistor. Based on the change in the electrical output, synthesized DNA and the viral DNA were detected.

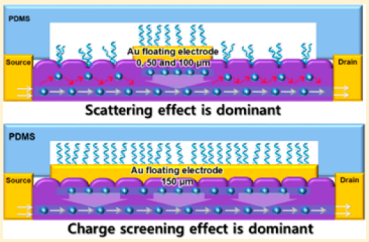

1. INTRODUCTION

Organic electronics have been extensively studied since the discovery of conducting polymers. Organic thin film transistors (TFTs) are employed as sensors due to their high sensitivity and biocompatibility, resulting from their structure and organic materials.[1] The TFT-based detection system has several advantages, including small size, fast response, can be integrated into arrays, and the low-cost of mass production. Organic electronic devices have also attracted attention due to their potential use in wearable sensors. Organic materials allow fabrication on flexible substrates using printers and at low temperature, which is profitable for wearable sensors.

A diversity of TFT-based biosensors have been employed for the specific sensing of biomolecules, such as proteins, enzymes, tumor cells, DNA, and so on.[2−4] Among the abundant biosensors, electrical DNA detection and characterization devices have surged in recent years. A number of electrical detection platforms have been reported for the analysis of DNA.[5] Indium gallium zinc oxide, silicon, and pentacene are some commonly employed active materials in the TFT-based sensors. Pentacene-based thin film transistors have gained a lot of attention as a sensor owing to their effortless fabrication process and biocompatibility.

In recent years, various research groups have reported a pentacene-based DNA detector.[6−8] Pentacene as an active layer is beneficial, as the DNA immobilizes on it without any surface treatment or modification. Although these structures have proven sensitive and effective, it limits the use of pentacene TFT for the detection of DNA only. Also, pentacene is known to be sensitive to moisture, which decreases the stability of the device. In this work, we fabricated a pentacene-based TFT with a floating electrode to detect viral DNA. A gold floating electrode was deposited on top of the pentacene active layer and thiolated polynucleotide probes were immobilized on the floating electrode to detect target DNA. The use of gold floating electrode can also extend the utility of this sensor to detect other biomolecules using thiolated probes. Recently, Chen et al. and Yan et al. reported a TFT, where they deposited the thiolated DNA on the source and drain electrode for the detection.[9,10] The deposition of DNA increased the contact resistance of the electrode, which was the basis of detection. A number of TFTs featuring an extended-bottom gate electrode have also been reported.[11−14] These devices are of some advantage as the gate electrode separates the sensing area from the TFT and increases the application of the device. However, they also rely on the change in the electrical properties of an extended gate electrode, which is considerably less sensitive. Contrarily, in our work, a floating electrode lies just over the active layer. Deposition of DNA or other charged biomolecules on the floating electrode alters the electric field of active area and modifies the distribution of carriers in the channel region. This results in a highly sensitive TFT for the detection of DNA. Recently, Kim et al. reported a CNT-FET with a gold floating gate electrode to deposit and detect DNA.[15] They suggested that the floating electrode forms a Schottky barrier with the active layer and deposition of DNA modulated the Schottky barrier by changing the work function. This changed the channel current and helped in detection of DNA.

Considering the benefits of organic material and floating electrode, in this work, we fabricated a pentacene based TFT with gold floating electrode to deposit and detect DNA. The floating electrode on the active layer helps with better alignment of DNA. Furthermore, a polydimethylsiloxane (PDMS)-based microfluidic channel was also integrated with the OTFT to make it a self-sustained sensor. The microfluidic channel helped in easy sample introduction, cleaning of the

Received: November 2, 2015
Revised: February 15, 2016
Published: February 17, 2016

DOI: 10.1021/acs.jpcc.5b10705
J. Phys. Chem. C 2016, 120, 4854−4859

active layer, insulating the OTFTs from external environmental factors and prevented DNA from binding to the pentacene or source/drain electrode. Microscopic and electrical analysis was performed to confirm the presence of DNA on the electrode. At the end, we will also discuss the principle governing the working of this sensor.

2. EXPERIMENTAL SECTION

2.1. Fabrication of Pentacene TFTs. Top contact pentacene-based TFTs fabricated on glass substrate were used for the study. Figure 1a shows the schematic of

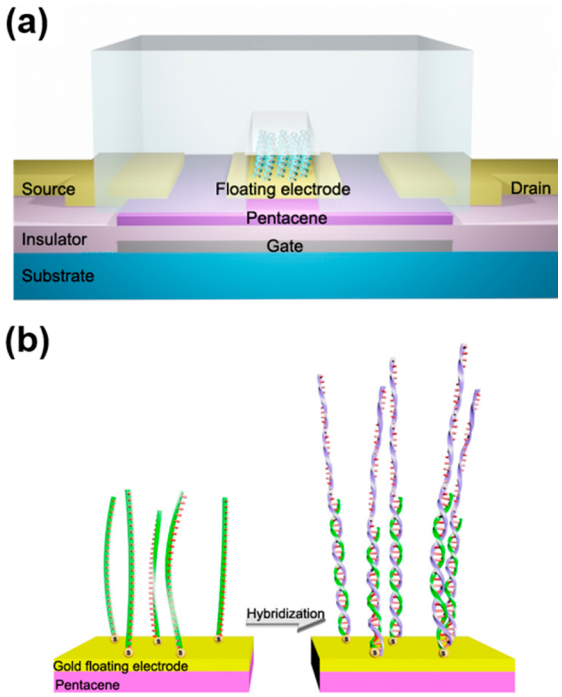

Figure 1. Schematic of microchannel integrated pentacene TFT with Au floating electrode. (a) Cross-sectional scheme of TFT and (b) immobilization of thiolated DNA probe and hybridization with target DNA on Au floating electrode.

microchannel integrated pentacene TFTs. For the fabrication, glass substrates were sequentially cleaned by ultrasonication in acetone, isopropyl alcohol, and deionized water for 20 min. At first, aluminum bottom gate electrode was deposited on the glass surface up to a height of 80 nm by thermal evaporation. PMMA gate insulator was then spin-coated and cured in a conventional oven at a temperature of 100 °C for 10 min to remove the solvent, followed by 160 °C for 30 min. For the active layer, pentacene was deposited to about 70 nm thickness through a patterned shadow mask in a high vacuum thermal evaporator at a rate of 0.1 Å/s, on the substrate at a temperature of 85 °C. The source/drain and Au floating electrode (of different width) were patterned to about 100 nm thickness by thermal evaporation using shadow mask defining a pentacene channel of width 1500 μm and length 250 μm. A negatively molded 150 μm wide PDMS microchannel was integrated on the final pentacene TFT, following the steps described in our previous work.[6]

2.2. Immobilization of DNA on the Au Floating Electrode. Single-stranded DNA (ssDNA) polynucleotide probes to capture target DNA were modified with thiol group and were dissolved and diluted with deionized (DI) water to the desired concentration. The thiolated DNA probes were immobilized on gold floating electrode, as depicted in Figure 1b. A total of 5 μL of thiolated ssDNA (30 mer, Poly-A, Bionics Inc., Korea) was injected into the microfluidic channel through the inlet and allowed to immobilize for the required time. Later, air was blown using a syringe to remove the leftover solution, and last, the device was subjected to drying for 30 min at room temperature. To carry out DNA hybridization, complementary nonthiolated ssDNA (30 mer, Poly-T) was injected to the Au floating electrode containing immobilized thiolated ssDNA. The hybridization proceeded for 1 h and then DI water was injected into the microfluidic channel for cleaning. After cleaning, the DNA immobilized pentacene TFT was dried for the measurement. The ssDNA probe and hybridized double-stranded DNA (dsDNA) on the floating electrode induced a charge in the active layer. The electrical performance of pentacene TFT was analyzed using 4145B source measure unit. Deposition and hybridization of DNA on bare pentacene were performed based on the steps described in our previous work.[16]

2.3. Lambda Phage Gene Preparation. To show the practicality of our sensor, we also detected the viral DNA. A *Hind* III digested lambda phage DNA purchased from Sigma-Aldrich was used for the analysis. For the capture and detection of DNA fragments, thiolated DNA probe was designed based on the lambda phage's genome sequence and restriction map. The sequence of the ssDNA probe was SH-TTC CAT GAC CGC ACC AAC AGG CTC CAA GCC, for capturing a 125 bp target fragment.

For the analysis of viral DNA, at first, the dsDNA digest was denatured to ssDNA by heating in a water bath at 95 °C for 5 min, followed by sudden chilling on ice for 10 min. Immobilization of the thiolated DNA probes, hybridization with denatured viral DNA, and measurement was performed as discussed in the previous section.

3. RESULTS AND DISCUSSION

3.1. Effect of DNA Solvents on the Channel Current. In order to make DNA solution, we first checked the effect of different solvents on the channel current. While phosphate buffer (PBS) and DI water are common solvent, a few groups have also used ethanol, to make the DNA solution.[17] Figure S1a–c shows the effect of buffer on the electrical performance of pentacene TFT. PBS and ethanol contain charged molecules, which changed the electrical output. The on-current decreased to 76% when ethanol was injected on the channel, whereas the off-current increased from $7.95 \times e^{-12}$ A to $5.84 \times e^{-8}$ A when PBS was injected. The DI water showed no significant changes in the electrical performance of the pentacene TFT after injection. Therefore, we used DI water throughout this study as the solvent for DNA.

3.2. Optimization of DNA Immobilization Time on Au Floating Electrode. To optimize the immobilization time of thiolated DNA probe on the Au floating electrode (width = 150 μm), we deposited ssDNA (30 mer poly-A) for different lengths of time (1, 12, and 24 h) and then measured the transfer and output characteristic of the pentacene TFT. Figure 2a shows the ratio of on-current (I_{DS}) as a function of drain voltage (V_{DS}, output characteristic; V_{GS} = −40 V) of the pentacene TFT. No change in the mobility was seen after the immobilization of DNA on the floating electrode (Figure S2a). The amount of threshold voltage shift and the ratio of I_{DS} of the

DOI: 10.1021/acs.jpcc.5b10705
J. Phys. Chem. C 2016, 120, 4854−4859

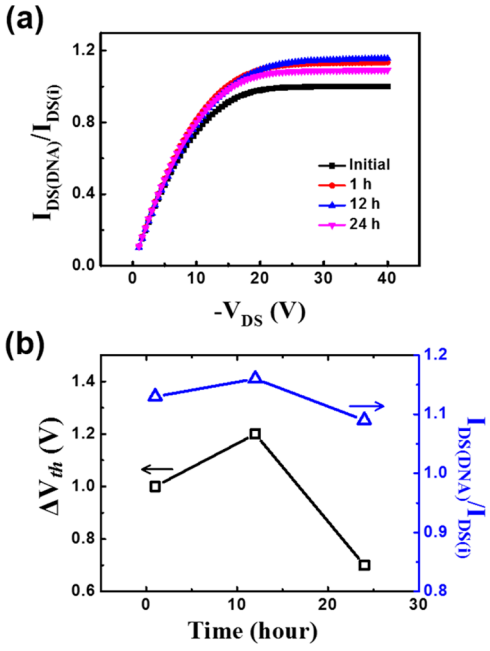

Figure 2. Optimization of DNA probe immobilization time on gold floating electrode. (a) Ratio of output characteristic of pentacene TFTs after probe immobilization (V_{GS} = −40 V) and (b) change of threshold voltage and current of pentacene TFTs.

device obtained after various DNA immobilization time on Au floating electrode is shown in Figure 2b. The threshold voltage of pentacene TFTs were extracted by fitting the linear part of $\sqrt{I_{DS}}$ versus V_G (Figure S2b). As the immobilization time increased, the device showed a more positive shift in the threshold voltage (V_{th}). The devices showed a saturation at 12 h, after which the performance decreased. The pentacene TFT reported a V_{th} of 1, 1.2, and 0.8 V, and the current changed by 13.4, 15.8, and 8.92% from the initial values for the immobilization time of 1, 12, and 24 h, respectively. An immobilization time of 12 h on the Au floating electrode was found to be optimal.

3.3. Detection of ssDNA and DNA Hybridization. The ssDNA molecules were immobilized on the Au electrode by thiol-Au chemistry. Figure 3a,b shows the transfer curve and output characteristics of the pentacene TFT after 100 μM of poly-A deposition. The transfer curve was plotted using root values to observe the threshold voltage shift. Immobilization of ssDNA induced a negative charge on the active layer. This caused an attraction of holes toward the surface and resulted in a positive shift of threshold voltage. In order to derive a correlation between the amount of DNA immobilization and the device response, a shift in the threshold voltage was also measured by varying the concentration of poly-A on the Au floating electrode. As the DNA concentration was increased, the ΔV_{th} also increased, Figure S3a. The error bar represents the standard deviation in the performance of three independent devices. Such an increase in ΔV_{th} was due to the increase in the concentration of DNA on the floating electrode, which collectively screens more holes from the channel region. The device could detect a minimum of 100 nM of the immobilized poly-A oligomer.

Detection of DNA hybridization on the Au floating electrode was performed by measuring the device performance before and after the hybridization of complementary DNA (100 μM, 30 mer poly-T) with the immobilized thiolated DNA probe (100 μM, 30 mer poly-A). The transfer and output characteristics of the pentacene TFT are shown in Figure 3a,b. The voltage shifted from −11.5 to −11.0 V, and the current increased from 4.97 to 5.41 μA for ssDNA to dsDNA, respectively. The hybridization of a complementary DNA further increased the negative charge on the floating electrode. This caused an increased attraction of holes toward the surface and resulted in a higher positive shift of the threshold voltage. In case of DNA immobilization on the bare pentacene surface,

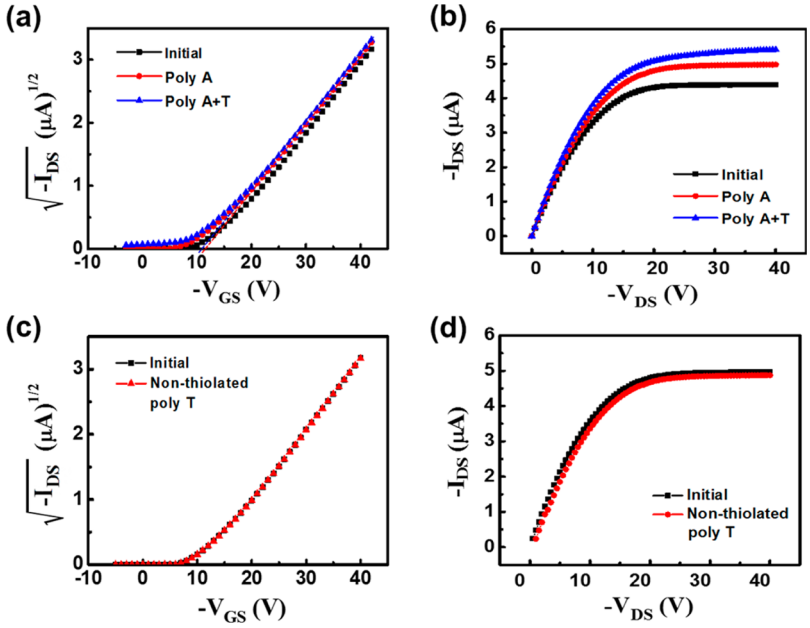

Figure 3. Electrical performance of pentacene TFT. (a) Transfer curve (V_{DS} = −20 V) and (b) output curve (V_{GS} = −30 V) of TFT before and after poly-A and poly-T hybridization on Au floating electrode. Intersection of dotted line represents the threshold voltage. (c) Transfer curve (V_{DS} = −20 V) and (d) output curve (V_{GS} = −30 V) of TFT after nonthiolated poly-T deposition on the Au floating electrode (negative control).

DOI: 10.1021/acs.jpcc.5b10705
J. Phys. Chem. C 2016, 120, 4854−4859

the nontarget DNA can also bind to the surface because of nonspecific physical and hydrophobic interaction. Compared with the bare pentacene TFT, the addition of floating electrode reduced the signal output; however, Au floating electrode offered higher selectivity.

To affirm the fact that only the immobilization of DNA brings a change in the sensor properties, we tried to deposit nonthiolated poly-T on the bare Au floating electrode and measured the device characteristics. Because of the absence of a linker, poly-T did not immobilize on the Au floating electrode; as a result, no change in the device characteristic was seen (Figure 3c,d). For a negative control and to check the selectivity of the sensor, we attempted the hybridization of poly-A and noncomplementary poly-C on the Au floating electrode. Figure S3b,c shows the transfer curve and the output curve of pentacene TFT before and after poly-A and poly-C hybridization. As expected, poly-C did not hybridize to the poly-A, resulting in no significant alteration in the electrical properties of pentacene TFT. The hybridization of DNA was also confirmed by the fluorescence imaging of TFT (Figure 4).

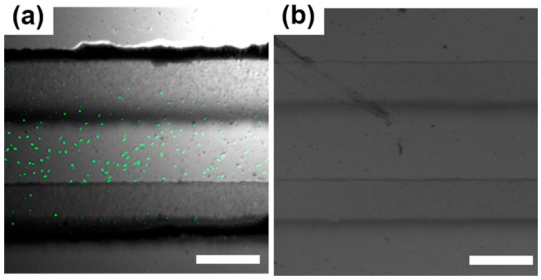

Figure 4. Confocal microscopic image of Au floating electrode with methylene blue treated (a) poly-A-T and (b) poly-A + poly-C. The bright green spots represent the hybridized dsDNA. Scale bar = 100 μm.

The devices were stained with methylene blue (MB) dye and observed under a confocal microscope. The green spots in Figure 4a represents the hybridized DNA (poly-A-T) on Au floating electrode; whereas, no fluorescence was seen when the hybridization of noncomplementary DNA was attempted Figure 4b). These fluorescence images confirm the specificity and selectivity of our sensor and that the change in pentacene TFT's performance is the result of DNA immobilization and hybridization. The bright individual spots of DNA rather than patchy fluorescence also prove that the Au floating electrode on active layer aids in better distribution and alignment of DNA.[6]

3.4. Detection of Viral DNA. Finally, as a proof of concept, we attempted to detect viral DNA through its hybridization with a probe-immobilized on the Au floating electrode. For this purpose, digested genomic DNA of lambda phage was used. To carry out the detection, at first, 100 μM of thiolated probe for viral DNA was immobilized on the Au floating electrode. Subsequently, the denatured product of 0.3 μg/μL of stock lambda phage DNA digest was injected on the electrode. The device was processed following the steps discussed in section 2.2. As seen from Figure 5, the device showed significant change in electrical properties in response to immobilization and hybridization of viral DNA. The positive shift in threshold voltage and increase in current was attained due to induced negative charge from the DNA. A higher increase in channel current, compared to that of poly-A-T, is seen here due to the hybridization of larger viral DNA fragment (125 bp). This

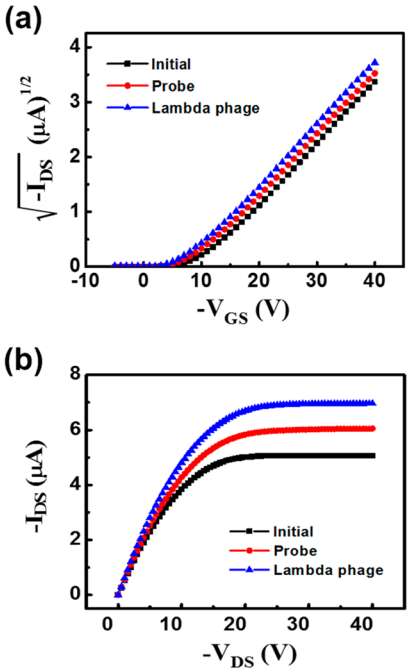

Figure 5. Detection of lambda phage DNA on Au floating electrode. (a) Transfer curve (V_{DS} = −20 V) and (b) output curve (V_{GS} = −30 V) of TFT after immobilization of thiolated probe and after hybridization with target lambda phage DNA.

result demonstrates the feasibility of our device as a disposable sensor for DNA hybridization and can lead to the development of a biosensor for rapid pathogen detection.

3.5. Effect of Electrode Dimension on DNA Sensing. To understand the effect of DNA on pentacene TFT with Au floating electrode, the devices with different dimensions of Au floating electrode were fabricated. The amount of immobilized DNA depends on the area of floating electrode. The width of three different Au floating electrodes were 50, 100, and 150 μm. The transfer curves of pentacene TFT without and with an Au floating electrode (150 μm), in the presence of DNA, are compared in Figure S4. The performance of different pentacene TFTs is also summarized in Table 1. The performance of

Table 1. Threshold Voltage (V_{th}) and Mobility (μ_{sat}) of Pentacene TFT with Different Structures, before and after DNA Immobilization

	DNA immobilization surface	initial	Poly-A	Poly-A-T
V_{th} (V)	pentacene	−11.5	−11.4	−11.4
	Au floating electrode (150 μm)	−11	−9.8	−9.2
μ_{sat} (cm^2/V·s)	pentacene	0.15	0.12	0.10
	Au floating electrode (150 μm)	0.17	0.17	0.17

pentacene TFTs after the DNA immobilization also depended on the dimension of electrode. Figure 6a shows the threshold voltage and mobility of device after immobilizing 100 μM of poly-A for 12 h on bare pentacene (electrode width = 0) and Au floating electrodes of different widths. Pentacene TFT without Au floating electrode showed a 0.3 cm^2/V·s reduction in mobility and no change in the threshold voltage (ΔV_{th} = 0). The pentacene TFT with 50 μm wide Au floating electrode presented a 0.4 V positive shift in threshold voltage and 0.105

DOI: 10.1021/acs.jpcc.5b10705
J. Phys. Chem. C 2016, 120, 4854−4859

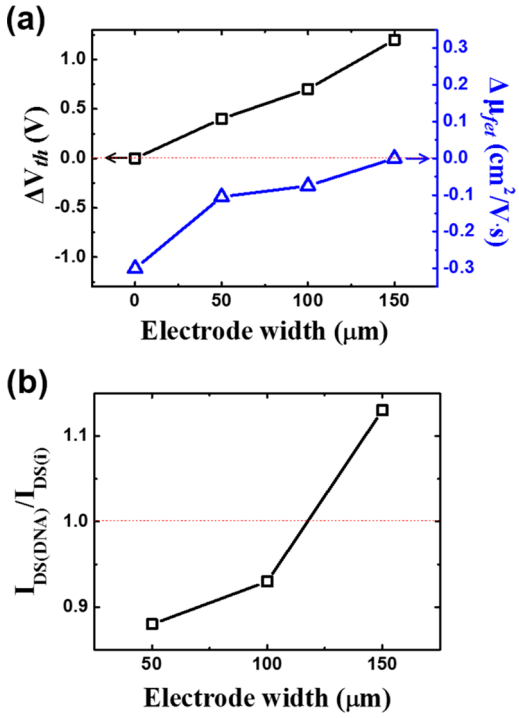

Figure 6. Electrical performance of pentacene TFT with Au electrode of different width, after DNA immobilization. (a) Change in threshold voltage and mobility. The width = 0 device represent the bare pentacene TFT. (b) Ratio of current obtained before and after DNA probe immobilization.

$cm^2/V{\cdot}s$ reduction in mobility. The 100 μm Au floating electrode showed a positive shift of about 0.7 V and mobility reduction of about 0.075 $cm^2/V{\cdot}s$. Contrarily, 150 μm Au floating electrode based TFT has no free pentacene surface to attach DNA, thus, showed no change in the mobility ($\Delta\mu_{fet}$ = 0), but a highest positive shift of about 1.2 V. When the DNA was immobilized on Au floating electrode, only the threshold voltage shifted; whereas, when on pentacene surface, only the saturation mobility decreased. The change in the channel current also followed the similar trend and is shown in Figure 6b.

3.6. DNA Sensing Mechanism. The mechanism of DNA sensing by the pentacene TFTs are shown in Figure 7. As per our previous work,[16] deposition of DNA on bare pentacene caused the scattering of holes in the pentacene grain boundary due to the negative charge of the DNA backbone (Figure 7a). Deposition of DNA on pentacene decreased the current mobility; however, the threshold voltage remained the same. In the present work, the pentacene TFT has an Au floating electrode on the pentacene active layer to immobilize thiolated DNA on it through chemical interaction. Figure 7b,c explains the charge screening effect of the device, as reported by Heller et al.[18] Immobilization of charged species induced a screening charge (doping) in the pentacene, thus, shifting the $I_{DS}-V_{GS}$ curve along the voltage axis. Therefore, only the pentacene TFT with 150 μm Au floating electrode showed the threshold voltage shift along with an increase in the channel current due to the screening effect of positively charged holes (Figure 7c), whereas 50 and 100 μm Au floating electrode showed decreased current because of the coupling of hole scattering effect and charge screening effect (Figure 7b). The DNA got adsorbed on the uncovered pentacene inside the microchannel,

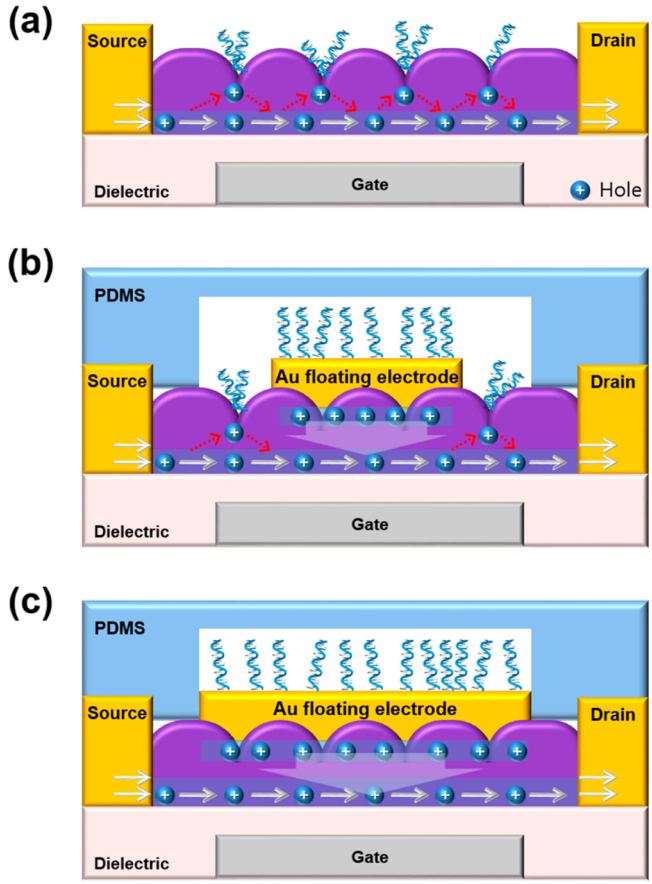

Figure 7. Effect of DNA immobilization on pentacene TFT. (a) DNA adsorbed on pentacene w/o floating electrode. The negative charged DNA causes holes scattering at the pentacene grain boundary. (b) DNA absorbed on pentacene surface and Au floating electrode (width < 150) results in combined hole scattering and screening charge effect. (c) DNA immobilized on Au floating electrode (width = 150) results in charge screening effect only.

which brought a change in the mobility and a decrease of current.

Figure 8 shows the relevant energy band structure of pentacene TFT with Au floating electrode and DNA

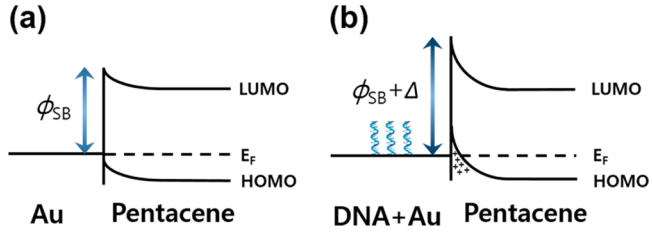

Figure 8. Band diagram of (a) Au/pentacene and (b) DNA bound/Au/pentacene OTFT.

immobilized on it. At the metal−semiconductor (M-S) junction interface, Schottky barrier is induced by the work function difference between Au and pentacene. The Schottky barrier, which is Φ_{SB}, creates a negligible amount of trap state at the interface, as shown in Figure 8a. However, after the DNA immobilization on Au floating electrode, the energy band structure changed due to the negative charge of DNA.[19,20] Figure 8b shows the energy band structure after DNA

DOI: 10.1021/acs.jpcc.5b10705
J. Phys. Chem. C 2016, 120, 4854−4859

immobilization. The negative charge of DNA increased the work function of Au floating electrode which induced the hole trap state due to higher Schottky barrier.[21] For this reason, the trap state at interface caused accumulation of holes in the pentacene and Au floating electrode interface. As a result, due to charge screening effect from accumulated holes, the threshold voltage decreased and the current increased as a back-bias effect.

4. CONCLUSION

In this work, thiolated ssDNA probe deposition and its hybridization was detected on the pentacene TFT with Au floating electrode. An additional floating electrode helped in protecting the active layer, and better alignment and specific detection of target DNA. The device could detect a minimum of 100 nM of the immobilized poly-A oligomer. Through this assay, the target gene of lambda phage viral DNA was captured and detected. The negative charge of the DNA attracted positive charge in the pentacene surface layer. As a result, the threshold voltage shifted toward positive and a small decrease in mobility was also seen. The amount of positive shift and increase in channel current depends on the concentrations and length of the DNA. It was confirmed by the device performance and an energy band diagram that the charge on DNA affects the carriers in the active layer, thereby altering the energy band of the materials. A future work will be directed to study the lower detection limit as well as increase the sensitivity of the sensor. This novel mechanism can be applied to the detection of DNA and other biomolecules, such as cell, enzyme, and so on.

■ ASSOCIATED CONTENT

Supporting Information

The Supporting Information is available free of charge on the ACS Publications website at DOI: 10.1021/acs.jpcc.5b10705.

Effect of DNA solvent, device optimization, and the response of DNA sensor (PDF).

■ AUTHOR INFORMATION

Corresponding Authors

*Phone: +82-31-299-4640. E-mail: rohitchand@skku.edu.

*Phone: +82-31-299-4323. Fax: +82-31-290-5828. E-mail: yongsang@skku.edu.

Author Contributions

†These authors contributed equally to this work.

Notes

The authors declare no competing financial interest.

■ ACKNOWLEDGMENTS

This work was supported by Business for Cooperative R&D between Industry, Academy, and Research Institute funded by Korea Small and Medium Business Administration in 2015 (Grant No. C0353887).

■ REFERENCES

(1) Lin, P.; Yan, F. Organic Thin-Film Transistors for Chemical and Biological Sensing. *Adv. Mater.* **2012**, *24*, 34−51.

(2) Cheng, S.; Hideshima, S.; Kuroiwa, S.; Nakanishi, T.; Osaka, T. Label-Free Detection of Tumor Markers Using Field Effect Transistor (Fet)-based Biosensors for Lung Cancer Diagnosis. *Sens. Actuators, B* **2015**, *212*, 329−334.

(3) Duan, X.; Li, Y.; Rajan, N. K.; Routenberg, D. A.; Modis, Y.; Reed, M. A. Quantification of the Affinities and Kinetics of Protein Interactions Using Silicon Nanowire Biosensors. *Nat. Nanotechnol.* **2012**, *7*, 401−407.

(4) Sang, S.; Wang, Y.; Feng, Q.; Wei, Y.; Ji, J.; Zhang, W. Progress of New Label-Free Techniques for Biosensors: A Review. *Crit. Rev. Biotechnol.* **2016**, 1−17.

(5) Veigas, B.; Fortunato, E.; Baptista, P. Field Effect Sensors for Nucleic Acid Detection: Recent Advances and Future Perspectives. *Sensors* **2015**, *15*, 10380−10398.

(6) Chand, R.; Jeun, J.-H.; Park, M.-H.; Kim, J.-M.; Shin, I.-S.; Kim, Y.-S. Electroimmobilization of DNA for Ultrafast Detection on a Microchannel Integrated Pentacene Tft. *J. Ind. Eng. Chem.* **2015**, *21*, 126−128.

(7) Gui, H.; Wei, B.; Wang, J. The Hybridization and Optimization of Complementary DNA Molecules on Organic Field-Effect Transistors. *Mater. Sci. Semicond. Process.* **2015**, *30*, 250−254.

(8) Zhang, Q.; Jagannathan, L.; Subramanian, V. Label-Free Low-Cost Disposable DNA Hybridization Detection Systems Using Organic Tfts. *Biosens. Bioelectron.* **2010**, *25*, 972−977.

(9) Chen, X.; Gui, H.; Wei, B.; Wang, J. A Label-Free Biosensor Based on Organic Transistors by Using the Interaction of Mercapto DNA and Gold Electrodes. *Mater. Sci. Semicond. Process.* **2015**, *35*, 127−131.

(10) Yan, F.; Mok, S. M.; Yu, J.; Chan, H. L. W.; Yang, M. Label-Free DNA Sensor Based on Organic Thin Film Transistors. *Biosens. Bioelectron.* **2009**, *24*, 1241−1245.

(11) Lin, P.; Luo, X.; Hsing, I. M.; Yan, F. Organic Electrochemical Transistors Integrated in Flexible Microfluidic Systems and Used for Label-Free DNA Sensing. *Adv. Mater.* **2011**, *23*, 4035−4040.

(12) Cao, Z.; Xiao, Z.-L.; Zhang, L.; Luo, D.-M.; Kamahori, M.; Shimoda, M. Molecule Counting with Alkanethiol and DNA Immobilized on Gold Microplates for Extended Gate Fet. *Mater. Sci. Eng., C* **2013**, *33*, 1481−1490.

(13) Lai, S.; Demelas, M.; Casula, G.; Cosseddu, P.; Barbaro, M.; Bonfiglio, A. Ultralow Voltage, Otft-Based Sensor for Label-Free DNA Detection. *Adv. Mater.* **2013**, *25*, 103−107.

(14) White, S. P.; Dorfman, K. D.; Frisbie, C. D. Label-Free DNA Sensing Platform with Low-Voltage Electrolyte-Gated Transistors. *Anal. Chem.* **2015**, *87*, 1861−1866.

(15) Kim, B.; Lee, J.; Namgung, S.; Kim, J.; Park, J. Y.; Lee, M.-S.; Hong, S. DNA Sensors Based on Cnt-Fet with Floating Electrodes. *Sens. Actuators, B* **2012**, *169*, 182−187.

(16) Kim, J.-M.; Jha, S. K.; Chand, R.; Lee, D.-H.; Kim, Y.-S. DNA Hybridization Sensor Based on Pentacene Thin Film Transistor. *Biosens. Bioelectron.* **2011**, *26*, 2264−2269.

(17) Kim, S. J.; Kim, B.; Jung, J.; Yoon, D. H.; Lee, J.; Park, S. H.; Kim, H. J. Artificial DNA Nanostructure Detection Using Solution-Processed in-Ga-Zn-O Thin-Film Transistors. *Appl. Phys. Lett.* **2012**, *100*, 103702.

(18) Heller, I.; Janssens, A. M.; Männik, J.; Minot, E. D.; Lemay, S. G.; Dekker, C. Identifying the Mechanism of Biosensing with Carbon Nanotube Transistors. *Nano Lett.* **2008**, *8*, 591−595.

(19) Kang, S. J.; Yi, Y.; Kim, C. Y.; Cho, S. W.; Noh, M.; Jeong, K.; Whang, C. N. Energy Level Diagrams of C60/Pentacene/Au and Pentacene/C60/Au. *Synth. Met.* **2006**, *156*, 32−37.

(20) Yeh, P.-H.; Li, Z.; Wang, Z. L. Schottky-Gated Probe-Free Zno Nanowire Biosensor. *Adv. Mater.* **2009**, *21*, 4975−4978.

(21) Koch, N.; Kahn, A.; Ghijsen, J.; Pireaux, J. J.; Schwartz, J.; Johnson, R. L.; Elschner, A. Conjugated Organic Molecules on Metal Versus Polymer Electrodes: Demonstration of a Key Energy Level Alignment Mechanism. *Appl. Phys. Lett.* **2003**, *82*, 70.

DOI: 10.1021/acs.jpcc.5b10705
J. Phys. Chem. C 2016, 120, 4854−4859